Extremophiles (2011) 15:281–291
DOI 10.1007/s00792-011-0356-5

ORIGINAL PAPER

Functional evaluation of four putative DNA-binding regions in *Thermoanaerobacter tengcongensis* reverse gyrase

Jie Li · Jingfang Liu · Jian Zhou · Hua Xiang

Received: 1 November 2010 / Accepted: 18 January 2011 / Published online: 12 February 2011

Abstract Reverse gyrase (RG) is an ATP-dependent type I DNA topoisomerase that introduces positive supercoils into DNA in thermophiles. Four regions of RG, i.e., the N-terminal zinc-finger motif, the β-hairpin in subdomain H1, the "latch", and the C-terminal zinc-finger motif, were predicted to be involved in DNA binding previously. In this paper, the functions of these regions in the enzymatic activity were evaluated by mutational analysis of the *Thermoanaerobacter tengcongensis* reverse gyrase (TtRG). We demonstrated that TtRG exhibited positive-supercoiling activity only at high temperature (>50°C) and low salt concentration ($\sim$30 mM NaCl), and three of these four regions (except for the "latch") were involved in DNA binding. Notably, mutations in the "latch" and β-hairpin regions of TtRG strongly impaired the ATPase activity, while mutations in the two zinc-finger motifs dramatically affected its thermal stability besides significant impairment of the DNA-binding ability. Accordingly, all of these four regions were found to be indispensable for the positive-supercoiling activity of TtRG. Taken together, we revealed that these putative DNA-contact regions affect the enzymatic activity of RG in different ways, and provided new insights into the structure and function of RG.

Keywords Reverse gyrase · DNA binding · Thermal stability · ATPase activity · *Thermoanaerobacter tengcongensis*

Communicated by L. Huang.

J. Li · J. Liu · J. Zhou · H. Xiang (✉)
State Key Laboratory of Microbial Resources,
Institute of Microbiology, Chinese Academy of Sciences,
No. 1 Beichen West Road, Chaoyang District,
100101 Beijing, People's Republic of China
e-mail: xiangh@sun.im.ac.cn

Introduction

DNA topoisomerases are important and indispensable enzymes to solve the problems of DNA entanglement that arise during processes of DNA transaction, including replication, transcription, recombination, repair, chromosome segregation and regulation of gene expression (Champoux 2001; Wang 2002; Schoeffler and Berger 2008; Hsieh and Plank 2009; Perugino et al. 2009). They use a tyrosine residue at the active site to reversibly cleave DNA by forming a transient tyrosyl phosphodiester bond. DNA topoisomerases are classified into two classes, depending on whether one strand (type I) or both strands (type II) of DNA are transiently broken to permit a change in topology (Brown and Cozzarelli 1979; Liu et al. 1980; Wang 1996; Champoux 2001). Type I topoisomerases are further classified into two subfamilies, type IA and type IB (Dekker et al. 2002).

Reverse gyrase is a peculiar type IA DNA topoisomerase, which introduces positive supercoils into DNA at the expense of ATP hydrolysis (Kikuchi and Asai 1984; Nakasu and Kikuchi 1985). It was first discovered in a hyperthermophilic archaeon, *Sulfolobus acidocaldarius* (Kikuchi and Asai 1984), and then found present in all hyperthermophiles (above 80°C) and in some thermophiles (65–80°C) (Brochier-Armanet and Forterre 2007; Perugino et al. 2009). Recently, several moderately thermophilic bacteria growing optimally at 55°C were also found containing a reverse gyrase gene, suggesting an adaptation to the extreme temperature fluctuations in the environment (Campbell et al. 2009). As a peculiar and hallmark protein for microorganisms living at high temperature, reverse gyrase may play an essential role in their growth in the harsh environments (Forterre 2002; Heine and Chandra 2009; Perugino et al. 2009). It has been reported that

reverse gyrase can protect DNA from damage at high temperatures as a heat-protective DNA chaperone or DNA renaturase (Kampmann and Stock 2004; Hsieh and Plank 2006), and that it is also involved in protecting DNA against physical or chemical damage (Napoli et al. 2004; Valenti et al. 2006). The reverse gyrase knockout mutant displays significant growth defects at high temperature, confirming its important role in thermoadaptation (Atomi et al. 2004).

The crystal structure analysis of *Archaeoglobus fulgidus* reverse gyrase has revealed that it comprises a helicase-like domain at its N-terminus and a type IA topoisomerase-like domain at its C-terminus (Rodriguez and Stock 2002). Four regions were predicted as potential DNA-binding sites, including the putative metal-binding site comprising three cysteines at the extreme N-terminus (a zinc-finger motif in other reverse gyrases), the β-hairpin (residues 201–217) that juts out from subdomain H1, the "latch"-like insertion (H3, residues 352–427) in subdomain H2, and the zinc-finger motif at the C-terminal domain (Rodriguez and Stock 2002). However, the functions of these regions especially in the enzymatic activity of reverse gyrase remain to be comprehensively characterized.

Genome sequence analysis of the thermophilic bacterium *T. tengcongensis* shows that it also encodes a reverse gyrase (TtRG, NP_623335.1) (Bao et al. 2002). In this study, the four corresponding regions in TtRG were individually mutated, and the enzyme properties in DNA supercoiling, DNA binding, ATPase activity and thermal stability were compared between wild-type TtRG and the mutants. Our results indicate that three of these four regions are actually involved in DNA binding, and two regions are related to ATP hydrolysis activity. Moreover, the two zinc-finger motifs are found to be important to the structure stability maintenance of TtRG at high temperature. Taken together, we provide novel evidences that these putative DNA-binding regions affect the enzymatic activities of reverse gyrase in different ways.

Materials and methods

Bacteria, plasmids and oligonucleotides

Escherichia coli DH5α was used as the host for cloning experiments, while *E. coli* BL21(DE3) was used for overexpression of the recombinant proteins. pET28a (Novagen) was used as the protein expression vector. The oligonucleotides used for gene amplifications and bandshift assays were listed in Tables 1 and 2. The *E. coli* strains were cultured at 37°C in Luria–Bertani (LB) medium with shaking. *T. tengcongensis* was grown in the modified MB medium at 75°C without shaking (Xue et al. 2001; Bao et al. 2002).

Cloning and mutagenesis

The reverse gyrase gene of *T. tengcongensis* was amplified with the primers P1/P2 (Table 1) from the genomic DNA by polymerase chain reaction (PCR), and inserted into the *Nco*I/*Sal*I site of the vector pET28a. The generated expression plasmid p28TtRG was used as a template for the following mutagenesis. Five TtRG mutants were generated (Fig. 1). Briefly, the mutant with deletion of the zinc-finger motif at the N-terminus (residues 1–34) was amplified with the primers P3/P2 (Table 1), whereas the mutants with deletions of the putative β-hairpin (residues 214–267) and the putative "latch" (residues 394–477) in TtRG were generated by PCR amplification using the overlap extension strategy as previously described (Horton et al. 1989; Rodriguez 2002), with the overlapping primers

Table 1 Primers used for gene amplification in this study

Names	Sequences (5′ to 3′)[a]	Purposes
P1	TCTACCATGGTGGCATTGGCAACAGGTG	P1/P2-p28TtRG
P2	CCGTGTCGACATTTTTTATTAGAATCTC	
P3	TCTACCATGGTGCCGTTTGAAGATGGAG	P3/P2-p28M1
P4	GCAGTTTTGAAACCAAAAGGCATAAAAC	P4/P5-p28M2
P5	TATGCCTTTTGGTTTCAAAACTGCATCT	
P6	TTTTGGGGAACTACATACATCCAGGCTT	P6/P7-p28M3
P7	CTGGATGTATGTAGTTCCCCAAAATACT	
P8	CAACTCCATAAAGCGTGCTAGTTCCGCTGGAGCTCAGTTTACAG	P8/P9-p28M4
P9	CTGTAAACTGAGCTCCAGCGGAACTAGCACGCTTTATGGAGTTG	
P10	GATGAACTACCCCGTGCTCCCTACGCTAATTCAGACAAGATTGAT	P10/P11-p28M4
P11	ATCAATCTTGTCTGAATTAGCGTAGGGAGCACGGGGTAGTTCATC	
P12	GAGCTAGGCTTTATAACTTTTCACAGAACAGACTCCAC	P12/P13-p28Y864F
P13	GTGGAGTCTGTTCTGTGAAAAGTTATAAAGCCTAGCTC	

[a] Restriction sites are underlined with single lines; the mutation sites are underlined with double lines

Table 2 Oligonucleotide sequences used for EMSA analysis

[a] DNA substrates used for EMSA analysis: single-stranded DNA, U1–U4; duplex DNA, U1–U4 annealed with the complementary D1–D4, respectively; duplex with single-stranded tail at 3′-end, U1 annealed with D2–D4, respectively; duplex with single-stranded tail at 5′-end, U1 annealed with D5–D7, respectively

Names	Sequences (5′ to 3′)[a]	Length (nt)
U1	GTTTTTTTAACTGGATAGCGGCAAAAAATTTTTATTTTATCCAGGTAATT	50
U2	GTTTTTTTAACTGGATAGCGGCAAAAAATTTTTATTTTAT	40
U3	GTTTTTTTAACTGGATAGCGGCAAAAAATT	30
U4	GTTTTTTTAACTGGATAGCG	20
D1	AATTACCTGGATAAAATAAAAATTTTTTGCCGCTATCCAGTTAAAAAAAC	50
D2	ATAAAATAAAAATTTTTTGCCGCTATCCAGTTAAAAAAAC	40
D3	AATTTTTTGCCGCTATCCAGTTAAAAAAAC	30
D4	CGCTATCCAGTTAAAAAAAC	20
D5	AATTACCTGGATAAAATAAAAATTTTTTGCCGCTATCCAG	40
D6	AATTACCTGGATAAAATAAAAATTTTTTGC	30
D7	AATTACCTGGATAAAATAAA	20

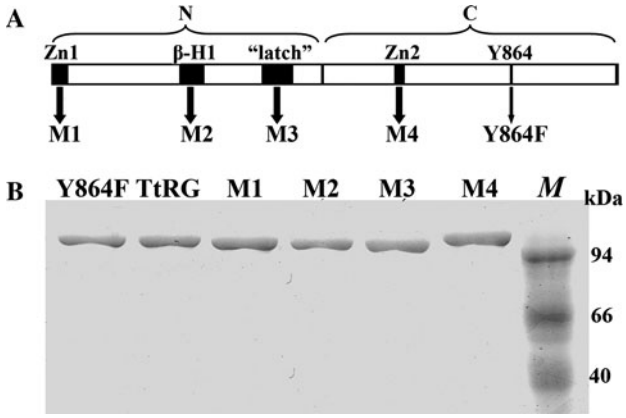

Fig. 1 Schematic diagram and SDS–PAGE analysis of wild-type TtRG and its mutants. **a** Schematic diagram showing the motif architecture of TtRG and two separate domains. The four putative DNA-binding regions in TtRG are indicated by *black boxes*. **b** SDS–PAGE analysis (12% acrylamide) of purified wild-type TtRG and its mutants (~5 μg each). *M* molecular mass markers (values in kDa on the right)

P4/P5 (for β-hairpin deletion) or P6/P7 (for "latch" deletion) partnered with primers P1/P2 (Table 1), respectively. These mutated fragments were digested and inserted into the *Nco*I/*Sal*I site of pET28a, resulting in the plasmids p28M1, p28M2 and p28M3. Mutation in the four cysteines of the zinc-finger motif at the C-terminal domain (residues 634–651) and mutant of the putative active site tyrosine (Y864F) were obtained respectively by site-directed mutagenesis as previously described (Li and Wilkinson 1997). Briefly, specific primers (P8–P11 for M4, P12/P13 for Y864F, Table 1) were designed for introducing desired mutations into p28TtRG with KOD-plus DNA polymerase (TOYOBO, Japan). The parental template DNA and the newly synthesized mutagenesis-primer-incorporated DNA were treated with *Dpn*I, and then transformed into *E. coli*. In this way, the p28TtRG derived plasmids of p28M4, p28Y864F were established. All the constructs were verified by DNA sequencing.

Protein expression and purification

The p28TtRG plasmid and its derivatives permit the production of recombinant proteins with a C-terminal His tag. The *E. coli* BL21(DE3) cells harboring these plasmids respectively were cultivated in LB media containing kanamycin (50 μg/ml) to reach OD600 of 0.4–0.6, at which point IPTG (isopropyl-β-D-thiogalactopyranoside) was added to a final concentration of 0.5 mM. The induced culture was allowed to grow for 16 h at 22°C. The cells were harvested by centrifugation and resuspended in lysis buffer containing 0.3 M NaCl, 10 mM imidazole, 50 mM sodium phosphate buffer (NaH_2PO_4/Na_2HPO_4, pH 8.0), and then lysed by ultrasonication. The lysates were centrifuged at 12,000 rpm for 30 min, and supernatants were purified first by a Ni^{2+}-nitrilotriacetate-agarose column (Novagen) and further by gel filtration chromatography with a Superdex 200 10/300 GL column (GE Healthcare) according to the manufacturer's instructions. Proteins were concentrated with Amicon Ultrafra-15 concentrators (Millipore) when necessary. The purified proteins were examined by SDS–PAGE, and the protein concentrations were determined by using a bicinchoninic acid (BCA) protein concentration assay kit (Pierce).

Reverse gyrase assay and protein thermostability assay

The standard reaction mixture (20 μl) for TtRG and its mutants contained 50 mM Tris–HCl, pH 7.5, 10 mM $MgCl_2$, 1 mM dithiothreitol, 0.5 mM EDTA, 30 μg/ml BSA, 5% glycerol, 30 mM NaCl, 1 mM ATP (or nucleotide indicated), and 0.5 μg of negatively supercoiled DNA (pUC18, New England Biolabs). A drop of mineral oil was added to cover the surface of the solution, and the reaction was initiated by immersing the reaction tube in a water bath set at 75°C, carried out for 45 min and terminated by adding 1/5 vol. of 5% SDS, 50 mM EDTA, 50% glycerol, 0.05% bromophenol blue. Products were analyzed using

1.2% one-dimensional (1D) or two-dimensional (2D) agarose gel electrophoresis with 3 μg/ml chloroquine in the second dimension. After electrophoresis, the gels were stained with ethidium bromide, photographed under UV light and quantified using the Quantity One software (Bio-Rad, USA). Each assay was performed at least three times. To determine the thermostability of wild-type TtRG and its mutants, the supercoiling assays were performed after the proteins had been pretreated at 75°C for the indicated time.

Electrophoretic mobility shift assay

The PAGE-purified oligonucleotides and their annealed DNA substrates used for electrophoretic mobility shift assay (EMSA) were listed in Table 2. Prior to annealing, upper-stream (U) oligonucleotides were radiolabelled at the 5′-end using [γ-^{32}P] ATP and T4 polynucleotide kinase. The annealing reaction mixture contained equimolar concentrations of two oligonucleotides in 50 mM Tris–HCl (pH 8.0), 10 mM $MgCl_2$, 50 mM NaCl, and 1 mM EDTA. The standard binding reaction mixture (20 μl) contained 50 mM Tris–HCl (pH 8.0), 10 mM $MgAc_2$, 30 mM NaCl, 1 mM DTT, 5% glycerol, 30 μg/ml BSA, 0.5 mM EDTA, 20 fmol labeled DNA probe, and the indicated amounts of appropriate proteins. After incubated for 20 min at 37°C or indicated temperatures, samples were immediately loaded on a non-denaturing 5% polyacrylamide gel (with an acrylamide/bisacrylamide weight ratio of 80:1) in 0.5× TBE buffer (preheated to 37°C or indicated temperatures) and run at 150 V for 2.5 h. Radioactivity was determined by autoradiography using an X-ray film and/or phosphorimaging and quantified using the ImageQuant software (Amersham). Each assay was performed in triplicate.

ATP hydrolysis assay

Unless otherwise stated, the ATPase assay reaction mixture (20 μl) contained 50 mM Tris–HCl (pH 8.0), 10 $MgCl_2$, 1 mM DTT, 30 μg/ml BSA, 200 pmol ATP (10 μM) with 1 μCi of [α-^{32}P] ATP (3,000 Ci/mmol) (PerkinElmer, USA), and 200 ng M13mp18 ssDNA (New England Biolabs). The reaction was initiated by addition of the protein at indicated concentrations. After 20-min incubation at different temperatures, the reaction was stopped by adding EDTA to 25 mM. Subsequently, 1 μl of the reaction mixture was spotted onto a polyethyleneimine cellulose sheet (TLC PEI-Cellulose F, Merck, Germany) and then developed with 1 M HCOOH and 0.5 M LiCl. The sheet was dried and exposed to an X-ray film and/or a phosphorimaging screen. The amount of the released ADP was quantified using the ImageQuant software. Each assay was performed in triplicate.

Results

Mutagenesis strategy and production of TtRG mutant

The *A. fulgidus* reverse gyrase crystal structure revealed four potential regions involved in DNA binding (Rodriguez and Stock 2002). By protein sequence alignment and 3D structure modeling analysis, these four corresponding regions in TtRG were identified (Fig. 1a). To functionally evaluate these regions in reverse gyrase, mutations were individually introduced into each of them as described in "Materials and methods", resulting in four mutant proteins named M1 (with the N-terminal 1–34 residues deleted), M2 (with the putative β-hairpin deleted at residues 214–267), M3 (with the putative "latch" deleted at residues 394–477), and M4 (with the four cysteines of the C-terminal zinc-finger motif at residues 634–651 replaced by alanines), respectively. Moreover, the putative active site tyrosine 864 was replaced by a phenylalanine (Y864F mutant). The wild-type TtRG and five mutant proteins were expressed in *E. coli* and purified to near homogeneity (Fig. 1b).

The biochemical properties of recombinant wild-type TtRG

All of the reverse gyrase proteins used in this study are His-tagged at their C-terminal ends, and we first examined the biochemical properties of the His-tagged wild-type TtRG. It was revealed that the supercoiling activity of TtRG was temperature dependent, and an efficient positive-supercoiling activity was observed at 75°C (Fig. 2a), the optimum growth temperature of *T. tengcongensis*. Notably, no supercoiling activity was observed below 50°C, suggesting that the purified TtRG was not contaminated by *E. coli* topoisomerases. Interestingly, the positive-supercoiling activity of TtRG was salt sensitive, which could only be detected at low salt concentrations, e.g., below 50 mM NaCl or 150 mM KCl, respectively (Fig. 2b).

The positive-supercoiling activity of TtRG was found to be dependent on ATP or its analogs (dATP and ATPγS), with ATP the most efficient (Fig. 3a). In contrast, when ATP was replaced by other NTP or dNTP cofactors, TtRG could only relax DNA to extremely relaxed status, but not positively supercoil it (Fig. 3a). In addition, without any cofactor in the assay, the enzyme could still partially relax the negatively supercoiled pUC18 DNA (−ATP in Fig. 3a). The final supercoiling extent depended on the stoichiometry of the TtRG protein to the DNA substrate. With the protein/DNA (P/D) molar ratio increasing, DNA substrate was more positively supercoiled in the presence of ATP (+ATP, Fig. 3b), and negative supercoiled DNA was more relaxed in the absence of ATP (−ATP, Fig. 3b).

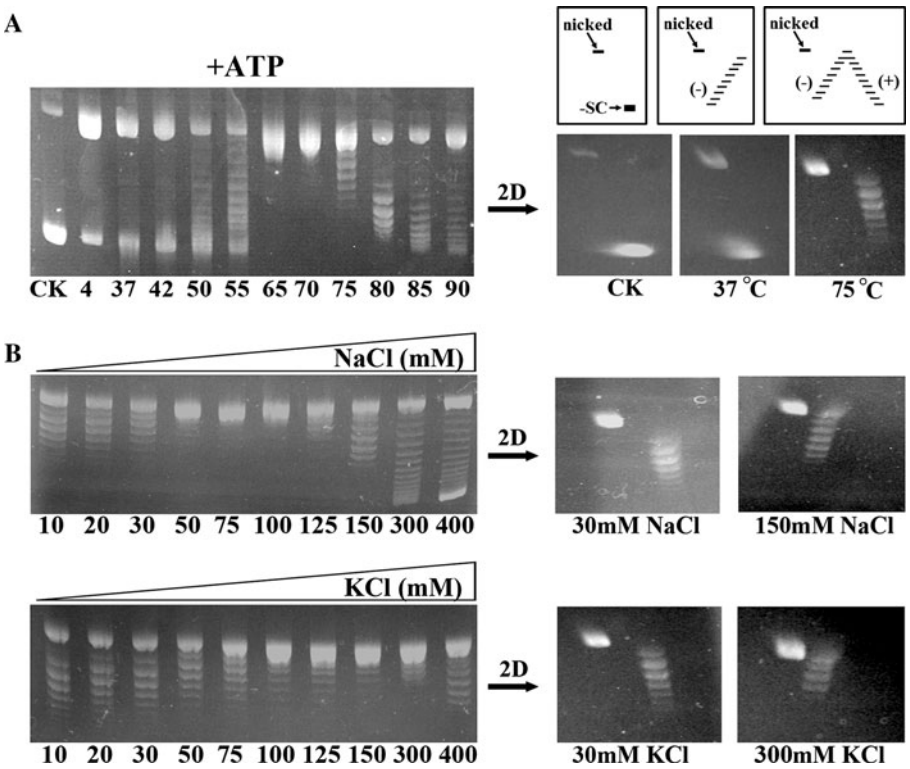

Fig. 2 Temperature and salt dependence of positive-supercoiling activity. *Lane CK* control reaction without enzyme. **a** Assays were performed at temperatures ranging from 4 to 90°C with ATP. One-dimensional (1D) and two-dimensional (2D) gel results with indicated temperature are shown. *Top right panel* schematic diagram of 2D gels, showing the migration of the negative supercoiled (−SC) and nicked DNA forms, as well as a complete arc of negative (−) to positive (+) topoisomers. **b** Assays were performed at different NaCl or KCl concentrations. 1D and 2D gel results with indicated salt concentrations are shown

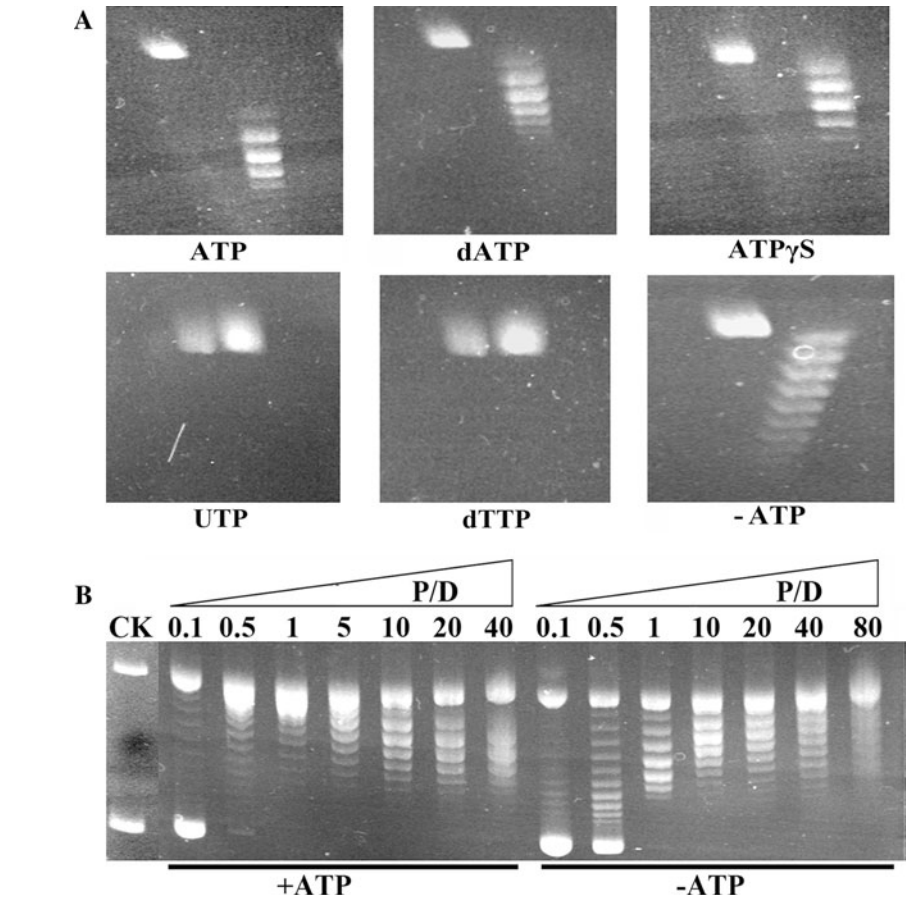

Fig. 3 Nucleotide and protein-to-DNA (P/D) molar ratio dependence of positive-supercoiling activity. *Lane CK* control reaction without enzyme. **a** Assays were set up in the presence of 10 mM of indicated nucleotides. 2D gel results are shown. **b** Assays were performed with indicated P/D ratios in the presence (+) or absence (−) of ATP. 1D gel results are shown

Accordingly, the standard supercoiling reactions of TtRG in the following assays were performed at 75°C in the presence of 1 mM ATP, 30 mM NaCl, and with a stoichiometric ratio (P/D) of 10, unless otherwise indicated.

The supercoiling activity of recombinant TtRG mutants

At the standard supercoiling reaction condition, the different mutant proteins were tested for their ability to produce positively supercoiled DNA (Fig. 4). As expected, the Y864F mutant totally lost the supercoiling activity, indicating that the 864th tyrosine is one important active site (Fig. 4).

Unexpectedly, the mutants M1, M2, M3 and M4 all totally lost the positive-supercoiling activity but maintained the negative-supercoil-relaxing activity (Fig. 4), suggesting that the four putative DNA-binding regions are all indispensable for the positive-supercoiling activity. As DNA binding and ATP hydrolysis activities of reverse gyrase play critical roles in the efficiency of its positive-supercoiling activity (Hsieh and Capp 2005; Jungblut and Klostermeier 2007; Bouthier de la Tour et al. 2008; Valenti et al. 2008), we investigated the contributions of these four regions in DNA binding and ATP hydrolysis activities by comparison of TtRG and the mutants in the following experiments.

Comparison of the DNA-binding ability of TtRG and its mutants

The DNA-binding property of wild-type TtRG was firstly analyzed using DNA substrates with different structures at 37°C (Fig. 5). Single or double-stranded DNA, or a 20-bp duplex region plus a single-stranded tail of 10–30 nt, were used as DNA substrates for DNA-binding analysis (Table 2). As shown in Fig. 5, the duplex DNA (40 or 50 bp) was bound with a slightly higher affinity than the single-stranded DNA (40 or 50 nt). Interestingly, when a 20-bp duplex DNA was flanked by a single-stranded DNA tail, it could be more efficiently bound by TtRG, especially with a tail longer than 10 nt (Fig. 5). These results were consistent with those of *A. fulgidus* reverse gyrase except that it requires a single-stranded tail longer than 20 nt to be efficiently bound (Rodriguez 2002).

Taking the optimal DNA substrate containing a 20-bp duplex with a 30-nt single-stranded tail at the 3′-end as a substrate, the DNA-binding ability of the mutants was analyzed at three different temperatures, 37, 55 and 75°C (Fig. 6a, b). Compared to wild-type TtRG, M1 bound DNA very weakly at all temperatures. Although some M1-DNA species were trapped in the wells (Fig. 6a), it is likely due to aggregation of this mutant protein but not real DNA-binding. Similarly, the binding activity of M4 was also significantly impaired (Fig. 6a, b). Although the binding ability of M2 was higher than that of M1 and M4, it was still much lower than that of wild-type TtRG, especially at high temperatures (Fig. 6a, b). Interestingly, the mutant M3 still bound DNA very efficiently, and its binding ability was even slightly higher than that of wild-type TtRG (Fig. 6a, b). These results suggested that three of the four regions, the two zinc-finger motifs and the β-hairpin, were indeed involved in DNA binding.

Comparison of ATPase activities of TtRG and its mutants

To compare the ATPase activities of wild-type TtRG and its mutants, the ATPase activity of TtRG was monitored

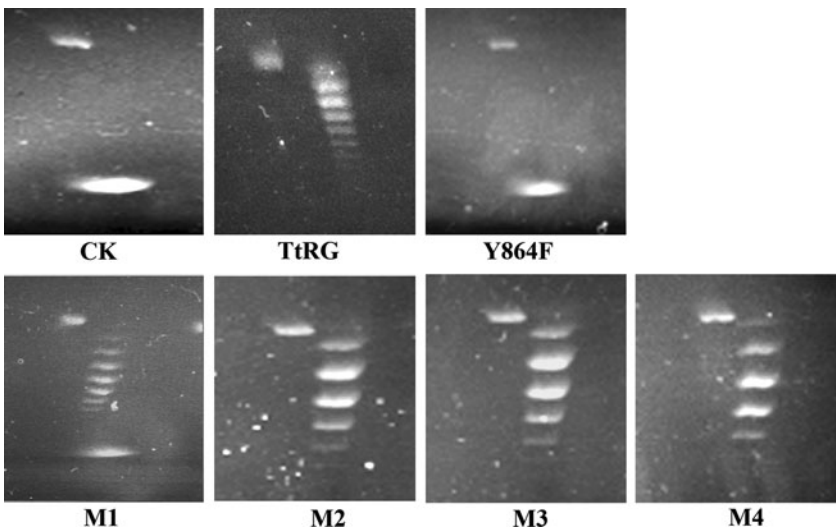

Fig. 4 Comparison of supercoiling activities of TtRG and its mutants. Assays were performed in a standard condition. 2D gel results are shown. *CK* control reaction without enzyme

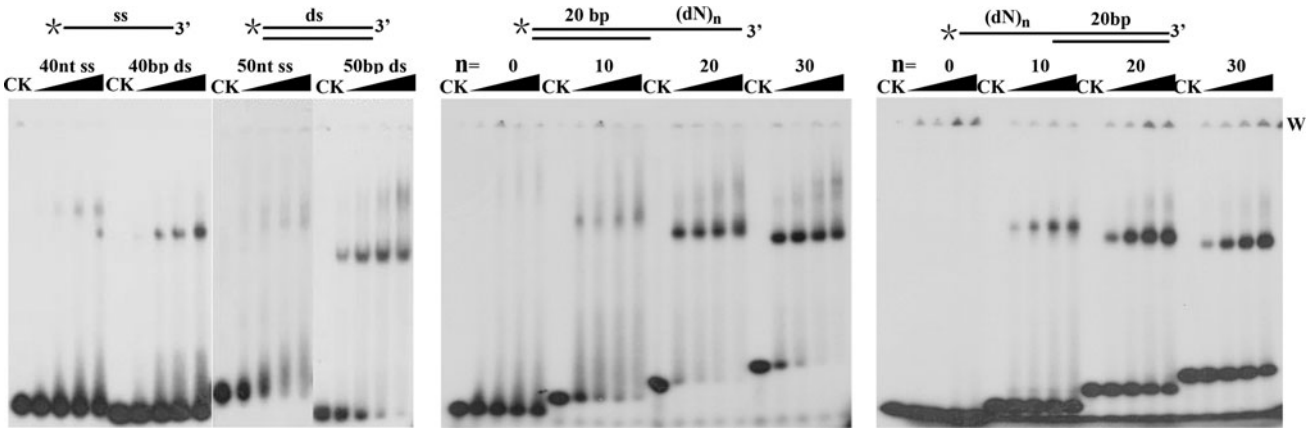

Fig. 5 Binding activity analysis of TtRG to DNA substrates with indicated structures. *ss* single-stranded DNA, *ds* duplex DNA, *n* the length of single-stranded tails flanking a 20-bp duplex. The *asterisk* denotes the ^{32}P-labeled end. Increasing amounts (50, 100, 150, and 300 nM) of purified wild-type TtRG were incubated with 20 fmol DNA substrates in standard reaction mixtures at 37°C for 20 min. *CK* control reaction without enzyme. *W* the position of the wells

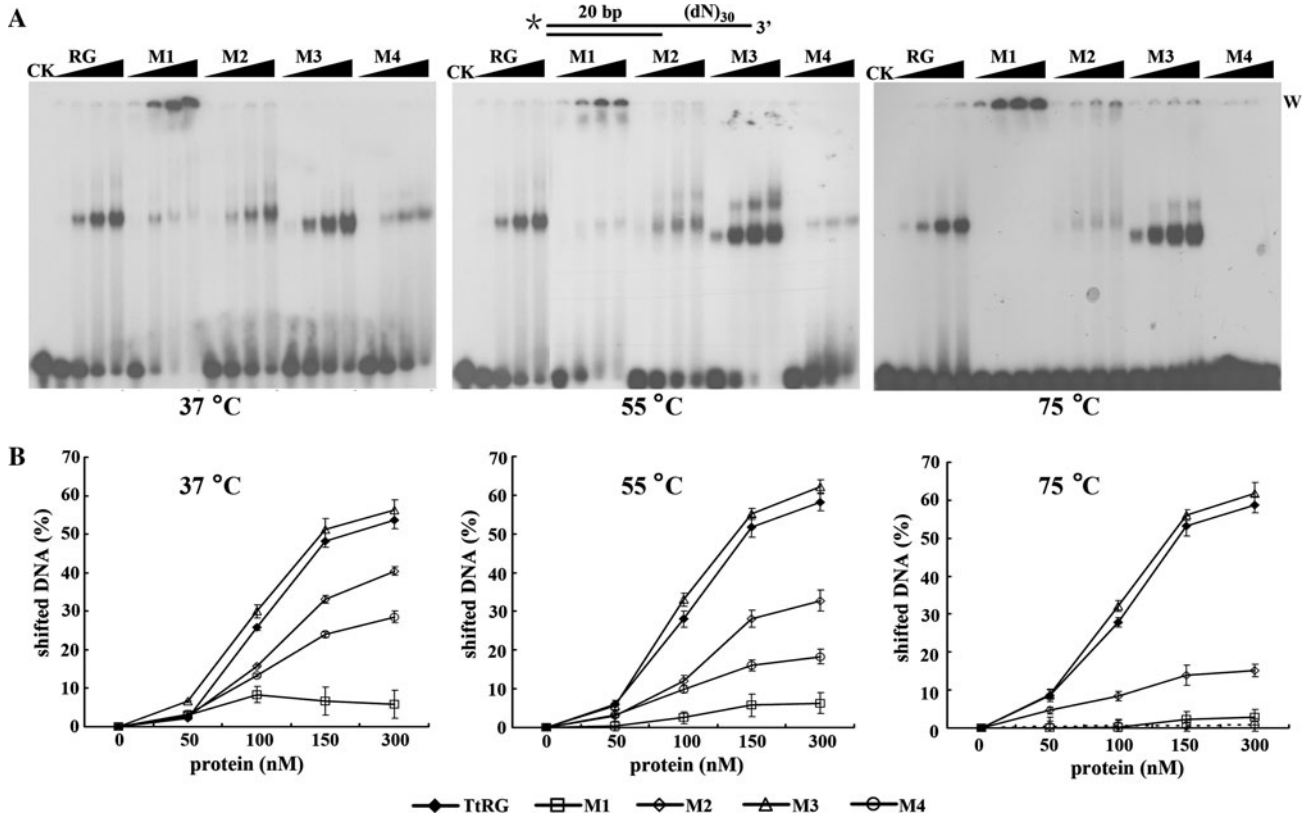

Fig. 6 Comparison of DNA-binding activities of TtRG and its mutants. **a** DNA-binding ability was compared between the mutants and wild-type TtRG at 37, 55, and 75°C, respectively. The DNA substrate containing a 20-bp duplex flanked by a 30-nt single-stranded tail at the 3′-end was used. *CK* control reaction without enzyme. *W* the position of the wells. **b** Quantification of the binding activity detected in (**a**). The fraction of shifted DNA versus the amount of protein used in the experiment is plotted. Each point represents the mean of three independent measurements

at first, using [α-^{32}P] ATP as the substrate. The reactions were performed at 37, 60, and 80°C in the presence of the single-stranded M13 DNA and different concentrations of TtRG. The released [α-^{32}P] ADP was measured, and the results showed an optimal ATPase activity at 60°C while a less efficient ATPase activity at 80°C (Fig. 7a).

Subsequently, the ATPase activity of the mutants was assayed at 60°C (Fig. 7). As shown in Fig. 7b, the ATP hydrolysis ability of M1 and M4 at 60°C was not

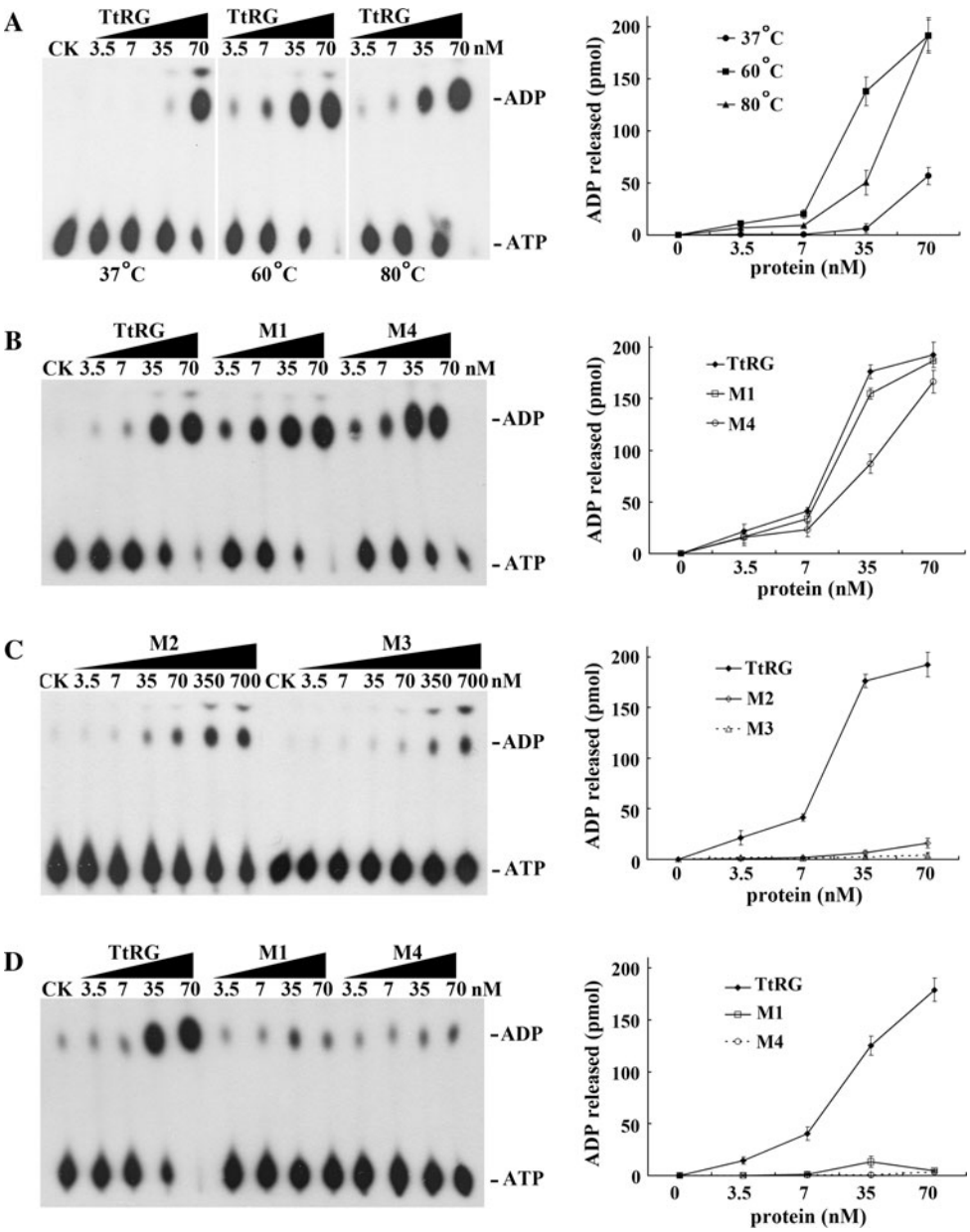

Fig. 7 ATPase activity comparison between wild-type TtRG and its mutants. Quantification of the assays is shown at the *right* of each panel. Each point represents the mean of three independent measurements. The background value corresponding to the released ADP in the assay without protein (*CK*) was subtracted from each value. **a** ATPase activity of wild-type TtRG detected at 37, 60, and 80°C. [α-^{32}P]ATP (10 μM) was used as the substrate, and was incubated with indicated concentration of TtRG. The released [α-^{32}P]ADP was measured using a standard assay. **b** Comparison of the ATPase activity between wild-type TtRG and the mutants M1 and M4 at 60°C. **c** ATPase activity of the mutants M2 and M3 at 60°C. **d** Comparison of the ATPase activity between wild-type TtRG and the mutants M1 and M4 at 80°C

significantly impaired. However, the ATPase activity of M2 was strongly impaired (Fig. 7c), and the ATP hydrolysis ability of M3 was almost abolished, which was still very weak even at a tenfold higher protein concentration (Fig. 7c). Interestingly, when the ATPase activities of M1 and M4 were examined at 80°C (Fig. 7d), the ATP hydrolysis ability of both mutants was significantly reduced, only slightly above background. Compared with that at 60°C, the significant impairment in the ATP hydrolysis ability of M1 and M4 at 80°C indicates that these two mutants might no longer be stable at 80°C. To reveal this possibility, we further tested and compared the thermal stability of TtRG and its mutants.

Comparison of thermal stabilities of TtRG and its mutants

After pretreatment at high temperature (75°C) for different time up to 60–180 min, DNA supercoiling activities of these proteins (as a reference of protein thermal stability) were examined in a standard assay condition. As shown in Fig. 8, the mutants M1 and M4 were highly unstable at 75°C (100% inactivation after 5-min pretreatment). However, the mutants M2 and M3 remained almost fully active after 1-h pretreatment, and their thermal stability was comparable with that of wild-type TtRG, which remained active after 3-h pretreatment (Fig. 8). These results

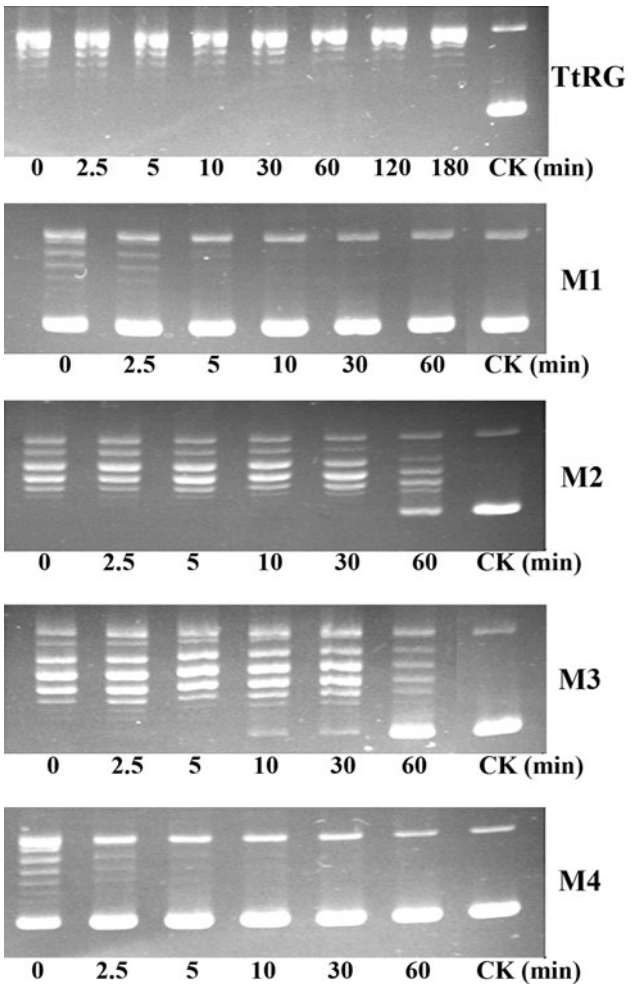

Fig. 8 Thermal stability comparison between TtRG and its mutants. After proteins had been pretreated at 75°C for indicated times, supercoiling assays were examined in a standard condition. 1D gel results are shown. *CK* control reaction without enzyme

indicated that the mutations in the two zinc-finger motifs, but not those in the β-hairpin and "latch" regions, greatly induced the loss of thermal stability of TtRG, suggested that the two zinc-finger motif regions are important for maintaining the structure stability of RG at high temperatures.

Discussion

In this paper, we present the first report on the significance of the four putative DNA-binding regions in enzymatic activity of reverse gyrase. A main conclusion from the mutational analysis of these four regions is that they play different roles in DNA binding, ATP hydrolysis and protein stability, but they are all essential for the positive-supercoiling ability of TtRG. This attests to the tight cooperation of DNA binding and ATPase activity with the supercoiling function of reverse gyrase.

TtRG is a typical reverse gyrase, which positively supercoils DNA in an ATP-dependent manner (Fig. 3a). This activity is temperature dependent (Fig. 2a) and salt sensitive (Fig. 2b). It preferentially binds to DNA substrates possess duplex region with single-stranded tail (Fig. 5), which are usually favored at high temperatures in negatively supercoiled DNA (Rodriguez 2002; Bouthier de la Tour et al. 2008). As other reverse gyrases (Shibata et al. 1987; Slesarev and Kozyavkin 1990; Rodriguez 2002; Bouthier de la Tour et al. 2008), the preferred binding to them might be an important reason for that the supercoiling activity of TtRG requires high temperature. TtRG also possesses an intrinsic ATPase activity (Fig. 7a) and it has a tyrosine active site (864th tyrosine) as all reverse gyrase (Fig. 4) (Nakasu and Kikuchi 1985; Slesarev and Kozyavkin 1990; Bouthier de la Tour et al. 1991; Rodriguez 2002; Hsieh and Capp 2005; Jungblut and Klostermeier 2007). Therefore, TtRG is a suitable model for studying the structure–function relationship of reverse gyrase.

Our mutational analysis revealed that the four putative DNA-binding regions of TtRG were all important for the positive-supercoiling activity (Fig. 4). But the changes in either DNA binding or ATP hydrolysis activity of these mutants were different. Mutagenesis in the two zinc-finger motifs and the β hairpin all dramatically impaired the DNA-binding ability (Fig. 6a, b), confirming that these three regions are important sites involved in DNA binding. An earlier study showed that site-directed mutagenesis in the N-terminal zinc-finger of *T. maritima* reverse gyrase led to a significant reduction in both the DNA-binding ability and the positive-supercoiling activity (Bouthier de la Tour et al. 2008). In comparison, the deletion of the N-terminal zinc-finger motif of TtRG led to a significant reduction in DNA binding and a complete loss of positive-supercoiling activity (Fig. 4). Because DNA binding plays a critical role in the efficiency of the positive-supercoiling reaction (Hsieh and Capp 2005; Valenti et al. 2008), it is conceivable that the reduction in the DNA-binding ability of the mutants (M1, M2 and M4) may impair their positive-supercoiling activity.

Interestingly, the DNA-binding activity of the "latch" mutant (M3) of TtRG is not affected (Fig. 6a, b), which is similar to the observation in *A. fulgidus* reverse gyrase (Rodriguez 2002, 2003), suggesting that the "latch" region was not directly involved in DNA binding for both reverse gyrases. However, notably, the ATPase activity of the M3 mutant of TtRG was strongly impaired (Fig. 7c), with the positive-supercoiling ability being completely abolished (Fig. 4). As the "latch" was predicted to participate in the conformational change of the whole enzyme upon binding of both nucleotide and DNA, resulting in the formation of the ATP hydrolysis pocket between the subdomains H1 and H2

(Rodriguez and Stock 2002), it is reasonable that mutations in this region affect the ATP hydrolysis pocket formation and impair the ATPase activity. Similarly, as β-hairpin lies in subdomain H1, deletion of the corresponding β-hairpin would also affect the pocket formation and impair the ATP hydrolysis activity consequently (Fig. 7c). Because the positive-supercoiling activity is strictly energy dependent, it is conceivable that impairment of ATP hydrolysis ability of M2 (the β-hairpin deletion) and M3 (the "latch" deletion) would lead to their loss of positive-supercoiling ability.

More significantly, the changes in protein thermal stability of the mutants corresponding to these four regions were different. The thermal stability of M2 (the β-hairpin deletion) and M3 (the "latch" deletion) was comparable to that of wild-type TtRG during 1-h incubation at 75°C (Fig. 8). However, the mutants M1 (the N-terminal zinc-finger mutation) and M4 (the C-terminal zinc-finger mutation) became very unstable at high temperatures, evidenced by the fact that their ATPase activity at 80°C was dramatically decreased compared to that at 60°C (Fig. 7b, d) and that they completely lost their enzyme activities after 5-min pretreatment at 75°C (Fig. 8). These results implied that the mutations in the two zinc-finger motifs induced the instability of TtRG at high temperature, and suggested that both zinc-finger motifs are important for maintenance of the structure thermostability of RG. This is the first report about the importance of the two zinc-finger motifs in maintaining the structure stability of reverse gyrase at high temperature, and highlights the importance of metal-ion chelating interactions by zinc-finger motif in thermostability as observed in other zinc-finger proteins (Sakai-Kato et al. 2009).

Taken together, our results provided novel evidences that three of the four putative DNA-binding regions of TtRG, except the "latch" region, were involved in DNA binding. In addition, both the "latch" and β-hairpin regions in TtRG were associated with the ATPase activity of TtRG, while the two zinc-finger motifs were important for DNA binding as well as the structure stability. Accordingly, impairment of the DNA-binding, ATPase activity or structural stability of the TtRG, would be the reasons of these four mutants completely lost their positive-supercoiling activities.

Acknowledgments This work was supported by grants from the National Natural Science Foundation of China (NSFC) (Nos. 30621005, 30925001).

References

Atomi H, Matsumi R, Imanaka T (2004) Reverse gyrase is not a prerequisite for hyperthermophilic life. J Bacteriol 186:4829–4833

Bao Q et al (2002) A complete sequence of the *T. tengcongensis* genome. Genome Res 12:689–700

Bouthier de la Tour C, Portemer C, Huber R, Forterre P, Duguet M (1991) Reverse gyrase in thermophilic eubacteria. J Bacteriol 173:3921–3923

Bouthier de la Tour C, Amrani L, Cossard R, Neuman KC, Serre MC, Duguet M (2008) Mutational analysis of the helicase-like domain of *Thermotoga maritima* reverse gyrase. J Biol Chem 283:27395–27402

Brochier-Armanet C, Forterre P (2007) Widespread distribution of archaeal reverse gyrase in thermophilic bacteria suggests a complex history of vertical inheritance and lateral gene transfers. Archaea 2:83–93

Brown PO, Cozzarelli NR (1979) A sign inversion mechanism for enzymatic supercoiling of DNA. Science 206:1081–1083

Campbell BJ et al (2009) Adaptations to submarine hydrothermal environments exemplified by the genome of *Nautilia profundicola*. PLoS Genet 5:e1000362

Champoux JJ (2001) DNA topoisomerases: structure, function, and mechanism. Annu Rev Biochem 70:369–413

Dekker NH et al (2002) The mechanism of type IA topoisomerases. Proc Natl Acad Sci USA 99:12126–12131

Forterre P (2002) A hot story from comparative genomics: reverse gyrase is the only hyperthermophile-specific protein. Trends Genet 18:236–237

Heine M, Chandra SB (2009) The linkage between reverse gyrase and hyperthermophiles: a review of their invariable association. J Microbiol 47:229–234

Horton RM, Hunt HD, Ho SN, Pullen JK, Pease LR (1989) Engineering hybrid genes without the use of restriction enzymes: gene splicing by overlap extension. Gene 77:61–68

Hsieh TS, Capp C (2005) Nucleotide- and stoichiometry-dependent DNA supercoiling by reverse gyrase. J Biol Chem 280: 20467–20475

Hsieh TS, Plank JL (2006) Reverse gyrase functions as a DNA renaturase: annealing of complementary single-stranded circles and positive supercoiling of a bubble substrate. J Biol Chem 281:5640–5647

Hsieh TS, Plank JL (2009) Helicase-appended topoisomerases: new insight into the mechanism of directional strand-transfer. J Biol Chem 284(45):30737–30741

Jungblut SP, Klostermeier D (2007) Adenosine 5′-O-(3-thio)triphosphate (ATPgammaS) promotes positive supercoiling of DNA by *T. maritima* reverse gyrase. J Mol Biol 371:197–209

Kampmann M, Stock D (2004) Reverse gyrase has heat-protective DNA chaperone activity independent of supercoiling. Nucleic Acids Res 32:3537–3545

Kikuchi A, Asai K (1984) Reverse gyrase—a topoisomerase which introduces positive superhelical turns into DNA. Nature 309: 677–681

Li S, Wilkinson MF (1997) Site-directed mutagenesis: a two-step method using PCR and DpnI. Biotechniques 23:588–590

Liu LF, Liu CC, Alberts BM (1980) Type II DNA topoisomerases: enzymes that can unknot a topologically knotted DNA molecule via a reversible double-strand break. Cell 19:697–707

Nakasu S, Kikuchi A (1985) Reverse gyrase; ATP-dependent type I topoisomerase from *Sulfolobus*. EMBO J 4:2705–2710

Napoli A et al (2004) Reverse gyrase recruitment to DNA after UV light irradiation in *Sulfolobus solfataricus*. J Biol Chem 279:33192–33198

Perugino G, Valenti A, D'Amaro A, Rossi M, Ciaramella M (2009) Reverse gyrase and genome stability in hyperthermophilic organisms. Biochem Soc Trans 37:69–73

Rodriguez AC (2002) Studies of a positive supercoiling machine. Nucleotide hydrolysis and a multifunctional "latch" in the mechanism of reverse gyrase. J Biol Chem 277:29865–29873

Rodriguez AC (2003) Investigating the role of the latch in the positive supercoiling mechanism of reverse gyrase. Biochemistry 42:5993–6004

Rodriguez AC, Stock D (2002) Crystal structure of reverse gyrase: insights into the positive supercoiling of DNA. EMBO J 21:418–426

Sakai-Kato K, Umezawa Y, Mikoshiba K, Aruga J, Utsunomiya-Tate N (2009) Stability of folding structure of Zic zinc finger proteins. Biochem Biophys Res Commun 384:362–365

Schoeffler AJ, Berger JM (2008) DNA topoisomerases: harnessing and constraining energy to govern chromosome topology. Q Rev Biophys 41:41–101

Shibata T, Nakasu S, Yasui K, Kikuchi A (1987) Intrinsic DNA-dependent ATPase activity of reverse gyrase. J Biol Chem 262:10419–10421

Slesarev AI, Kozyavkin SA (1990) DNA substrate specificity of reverse gyrase from extremely thermophilic archaebacteria. J Biomol Struct Dyn 7:935–942

Valenti A, Napoli A, Ferrara MC, Nadal M, Rossi M, Ciaramella M (2006) Selective degradation of reverse gyrase and DNA fragmentation induced by alkylating agent in the archaeon *Sulfolobus solfataricus*. Nucleic Acids Res 34:2098–2108

Valenti A et al (2008) Dissection of reverse gyrase activities: insight into the evolution of a thermostable molecular machine. Nucleic Acids Res 36:4587–4597

Wang JC (1996) DNA topoisomerases. Annu Rev Biochem 65:635–692

Wang JC (2002) Cellular roles of DNA topoisomerases: a molecular perspective. Nat Rev Mol Cell Biol 3:430–440

Xue Y, Xu Y, Liu Y, Ma Y, Zhou P (2001) *Thermoanaerobacter tengcongensis* sp. nov., a novel anaerobic, saccharolytic, thermophilic bacterium isolated from a hot spring in Tengcong, China. Int J Syst Evol Microbiol 51:1335–1341